

Article

# Electrochemical Deposition of Ni–W Crack-Free Coatings

Dmitriy V. Suvorov <sup>1</sup>, Gennady P. Gololobov <sup>1</sup>, Dmitriy Yu. Tarabrin <sup>1</sup>, Evgeniy V. Slivkin <sup>1</sup> ,  
Sergey M. Karabanov <sup>1</sup> and Alexander Tolstoguzov <sup>1,2,3,\*</sup> 

<sup>1</sup> Centre for Advanced Technologies and Materials, Ryazan State Radio Engineering University, Gagarin Str. 59/1, Ryazan 390005, Russia; dmitriy\_suvorov@mail.ru (D.V.S.); gololobov.gennady@yandex.ru (G.P.G.); tarabrin-dmitriy@mail.ru (D.Y.T.); e.slivkin@mail.ru (E.V.S.); smkarabanov.rsreu@gmail.com (S.M.K.)

<sup>2</sup> Centre for Physics and Technological Research (CeFITec), Departamento de Física da Faculdade de Ciências e Tecnologia, Universidade Nova de Lisboa, 2829-516 Caparica, Portugal

<sup>3</sup> Key Laboratory of Artificial Micro- and Nano-Materials of Ministry of Education, School of Physics and Technology, Wuhan University, Wuhan 430072, China

\* Correspondence: a.tolstoguzov@fct.unl.pt; Tel.: +7-960-577-7900

Received: 1 June 2018; Accepted: 25 June 2018; Published: 30 June 2018



**Abstract:** The main features of electrochemical deposition of coatings based on Ni–W binary alloy in the pulse current mode using pyrophosphate electrolytes were studied. Two electrolytes with a pH of 8.7 and 9.5 were used. The deposition was carried out with the current density varying in the range of 0.01–0.1 A·cm<sup>−2</sup>, and the duty cycle (the relative pulse duration) was changed within the range 20–100%. The surface morphology and elemental and phase composition of the coatings were studied by scanning electron microscopy, energy-dispersive X-ray microanalysis and X-ray diffractometry. The experimental conditions allowing us to achieve the maximum Faradaic efficiency and W content in the coatings were determined. It was found that the pulse current mode enabled the fabrication of crack-free coatings with a thickness greater than 6 μm.

**Keywords:** Ni–W binary alloy; crack-free coatings; electrodeposition; pulse current mode; Faradic efficiency; pyrophosphate electrolyte

## 1. Introduction

Electrodeposited metal and alloy coatings are widely employed to increase surface hardness, electroconductivity, wearability, corrosive and electroerosive resistance, to provide necessary decorative properties, etc. Among them, molybdenum and tungsten alloys with metals of the iron group, in particular Ni–W alloys, are regarded as very promising electrolytic coatings possessing good operating characteristics, especially electroerosive resistance [1–3]. The microhardness of these alloys depends on the relative W content and can reach 4.5–7 GPa. After the heat treatment this value increases to 9–10 GPa.

Binary Ni–W coatings could be a good substitute for hard chromium plating. As compared with Cr coatings, Ni–W coatings keep their hardness at elevated temperatures and exhibit higher corrosive and wear resistance [4,5]. Moreover, the deposition of Ni–W coatings is a nontoxic and environmentally friendly process [6,7], and it is less energy-consuming [8] than Cr electroplating technology.

The field of application of Ni–W electrodeposited coatings is vast [9]. For example, the proper corrosion resistance of these alloys has made possible their application as hard coatings [10–19]. It is known [20–22] that Ni–W alloys exhibit catalytic activities [20–22] and can be employed as catalysts for the oxidation of exhaust gases of internal combustion engines.

In electrical contacts, it is necessary to have effective barrier layers against corrosion and diffusion. Because nanocrystalline Ni–W can improve the corrosion resistance, minimize contact wear, and significantly reduce the formation of intermetallic compounds resulting from interlayer diffusion at interfaces, these alloys with 15.8 at.% of tungsten can be considered reasonably effective barriers for electronic/electrical contacts [23].

One of the main problems with electroplating technology is a high level of internal stress in the deposited coatings, causing damage (cracks). Using water-based electrolytes for Ni–W electroplating, one can observe significant hydrogen release, resulting in the distortion of coating structure due to its hydrogen saturation, which provokes the stress cracking of coatings. These microcracks significantly influence the operating characteristics of coatings, particularly their corrosion resistance [9]. To avoid crack development, different methods are used like introduction of special additives to electrolytes, application of the pulse current mode, employing a third co-precipitating metal, and deposition under supergravitation conditions [24].

In [24], the influence of the electrolytes with different ligands (citrate, glycine, triethanolamine, and their combinations) as well as the regimes of electrochemical deposition (DC and the pulse mode with reverse current) on the level of internal stresses in Ni–W coatings was studied. It was shown that in all cases internal stress in the coatings increases with the time from the beginning of deposition. To decrease internal stress, a complex electrolyte containing the three abovementioned ligands in equal proportions was proposed. Pulse-reverse current mode somewhat decreased such stresses, but did not prevent their development over the course of time. At the same time, adding 1, 3, 6 naphthalene trisulfonic acid and insertion of chloride ions in electrolytes by substituting nickel sulphite for its chloride compound along with application of the pulse-reverse current mode significantly reduced the probability of cracks developing in coatings. However, in that case the coatings exhibited high surface roughness and rather low W content (ca. 7–9 at.%), which limits their range of application.

It was shown [25] that electrochemical deposition of Ni–W alloys from citrate electrolytes under the conditions of high gravitation (within the range of 101–256 g) suppresses crack development. Effective removal of hydrogen bubbles from the coating surface by means of increased Archimedean force is considered the main mechanism responsible for improving the coatings' quality.

A comparative study of electrochemical deposition of Ni–W alloys from citrate electrolytes under the DC and pulse current (PC) modes was carried out in [26]. It was revealed that the PC mode promotes an increase of W content as compared to the DC mode, and a significant decrease of the surface roughness of coatings was achieved under a duration of cathode pulse of 1 millisecond (at the ratio of cathode pulse duration to the pause as 1/10).

Well-proved citrate electrolytes on a base of organic ligands glycine and triethanolamine are widely employed for the fabrication of Ni–W coatings. However, their use is not always possible due to the aggressive interaction of citrate and citric acid with substrate materials.

The main disadvantages of these electrolytes are the following:

- The deterioration of the coatings' adhesion due to the formation in electrolytes of the products of anodic oxidation of ligands' ions;
- The presence in the coatings of carbon-containing organic impurities, which can cause carbon diffusion towards the surface of coatings;
- The rather low stability of the electrolyte composition.

Among various electrolytes with inorganic ligands, pyrophosphate electrolytes can be employed for the production of coatings on the base of refractory metals, including Ni–W coatings. The main advantages of such electrolytes are their stability, an absence of anodic oxidation of ligands ions, the high scattering power, an ability to produce "smooth-faced" coating (with low surface roughness), carbonless composition of electrolytes, and environmental safety. However, the features of electrochemical deposition of Ni–W alloys from pyrophosphate electrolytes are insufficiently

investigated. For example, in [27,28] the deposition of these alloys in DC mode was studied but the presence of surface cracks in coatings was revealed.

One should point out that the processes occurring on an electrode during electrodeposition are very complex. They include ion transfer towards the surface of electrode, direct discharge of ions, formation of new substances and many others. One of the important factors promoting the formation of the deposited film is the surface charge of the electrodeposited materials and substrate. This surface charge is mainly associated with the isoelectric point of the materials and the variation in the local pH over the course of deposition. In our opinion, an approach that considers the surface charge and is based on the use of schematic zeta potential curves [29] provides rather good results in the case of deposition of colloidal particles from solution but cannot be considered as a key criterion for the electrodeposition of Ni–W coatings on copper substrate studied in our work.

The present work studies the electrochemical deposition of Ni–W binary alloys using pyrophosphate electrolytes in the pulse current mode and, based on the results of this study, reveals the main features of the fabrication of crack-free coatings.

## 2. Materials and Methods

Binary Ni–W alloy was electrochemically deposited from a pyrophosphate–ammonium electrolyte [28] containing NiSO<sub>4</sub>·6H<sub>2</sub>O (nickel sulphate hexahydrate) 0.2 M, Na<sub>2</sub>WO<sub>4</sub> (sodium tungstate) 0.2 M, K<sub>4</sub>P<sub>2</sub>O<sub>7</sub> (potassium pyrophosphate) 0.6 M, and (NH<sub>4</sub>)<sub>2</sub>SO<sub>4</sub> (ammonium sulphate) 0.15 M. All these components are dissolved in bi-distilled water with resistivity of 1 MΩ·cm. Two electrolytes with different pH, namely 8.7 and 9.5, were used. Such a choice is determined by the range of electrolyte stability (8.5–10.0) and by significant differences in the ligand content of electrolytes depending on the pH value [28]. This value was adjusted by means of adding H<sub>2</sub>SO<sub>4</sub> (0.1 M solution) and NaOH (0.1 M solution). Pyrophosphate ions P<sub>2</sub>O<sub>7</sub><sup>4−</sup> form complex ions with Ni<sup>2+</sup> ions of Ni(P<sub>2</sub>O<sub>7</sub>)<sub>2</sub><sup>6−</sup> composition, and the addition of NH<sub>4</sub><sup>+</sup> ions significantly increases the Faradaic efficiency [27]. The volume in each experiment was 250 mL.

The acidity of electrolytes was monitored with a multiparameter pH Meter HI 2020 by Hanna Instruments (Woonsocket, RI, USA). Even in the longest experiment (6 h in duration), the pH value changed by no more than 0.1. Such variation could not appreciably influence the results of our experiments.

An usual two-electrode cell was used in our experiments. As substrates, oxygen-free copper Cu-DHP plates with a size of 1 × 2 cm<sup>2</sup> and a thickness of 1 mm were employed. Substrates were polished by means of a felt circle without any abrasive and then were degreased in a solution containing NaOH and Na<sub>2</sub>CO<sub>3</sub> at a concentration of 100 g·L<sup>−1</sup> for each component at the temperature of 70 °C. Before electrochemical deposition, substrates were immersed in a 15% solution of HCl for 30 s and then washed in bi-distilled water. As an anode, a 4 cm<sup>2</sup> platinum plate was used. The current density ranged within 0.01–0.1 A·cm<sup>−2</sup>, and both DC and PC modes were applied. The pulse repetition period did not change and was 100 ms; the cathode pulse duration varied within 20–50 ms, and the pause duration was chosen in the range of 50–80 ms. A potentiostat IPC Pro 3A by Volta (St. Petersburg, Russia) was employed to provide the electrical currents during electrodeposition.

The electrolyte's temperature in our experiments was 55 ± 1 °C. It was provided by means of a magnetic stirring with heating C-MAG HS 7 digital by IKA (Staufen, Germany) using the feedback via a temperature sensor PT1000 by Thermometrics (Northridge, CA, USA). Stirring of the electrolyte was not performed.

Microstructural images were collected using a scanning electron microscope JSM-6610LV by JEOL (Tokyo, Japan) equipped with an energy-dispersive X-ray microanalyzer INCA X-MAX by Oxford Instruments (Abingdon, Oxfordshire, UK), which allowed for determining quantitative elemental composition of the coatings. We used a 30 keV acceleration potential in our experiments. The thickness of coatings was determined by means of cross-section microstructural measurements on the scanning electron microscopy (SEM) images. The relative accuracy of these measurements was estimated within

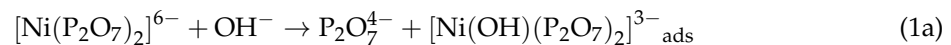
the range of  $\pm 3.5\%$ . The phase composition of the coatings was studied by X-ray diffractometer D8 Discover by Bruker (Billerica, MA, USA) at the Research Centre “Physics and technology of micro- and nanostructures” of the Institute for Physics of Microstructures of the Russian Academy of Science (Nizhny Novgorod, Russia).

### 3. Results and Discussion

During our experiments more than 150 coatings with different thicknesses using two electrolytes with a pH of 8.7 and 9.5 were produced and studied. The electrochemical deposition was carried out in the DC and PC modes for different current densities.

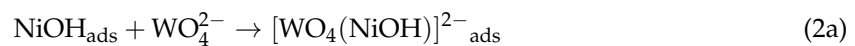
Below we consider the chemical reactions taking place in the course of Ni–W deposition from pyrophosphate electrolytes [27,28].

The nickel reduction occurs via a three-stage reaction:

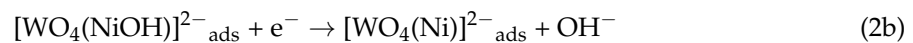


In the first stage, a complex pyrophosphate ion  $[\text{Ni}(\text{P}_2\text{O}_7)_2]^{6-}$  interacts with hydroxide ion  $\text{OH}^-$ , which results in the formation of complex ion  $[\text{Ni}(\text{OH})(\text{P}_2\text{O}_7)_2]^{3-}$ . This ion is adsorbed on the surface of the growing coating. In the second stage, it is reduced to  $\text{NiOH}$ , which in turn is reduced to metallic nickel.

In accordance with [28], co-precipitation of tungsten occurs via the chemical reaction, resulting in the formation of a cluster heterometallic compound containing an Ni–W bond:



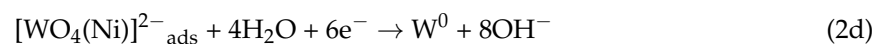
This compound is reduced by means of one of the reactions:



or



In the compounds formed, the W–O bond is very weak, and these compounds are reduced to tungsten on the cathode:



Representative SEM images of Ni–W coatings produced in the DC mode with different current densities are presented in Figure 1. Inserts in the upper right corner in both panels of this figure show energy-dispersive X-ray spectra (EDS). The pH in both cases was 9.5, and a thickness of the coatings was ca. 6  $\mu\text{m}$ . In these figures, one sees a rather dense net of microcracks on the surface, resulting either from hydrogen embrittlement or residual stress [30,31]. This net is formed in a stochastic manner and coincides with globule boundaries, but only for some fragments. Also, the number of cracks and W content increase with an increase in the current density. As mentioned in [1,2,28], a coating of a thickness bigger than 5  $\mu\text{m}$  is practically impossible to prepare without cracks using the DC mode.

### 3.1. Influence of the Conditions of Electrochemical Deposition on the Faradaic Efficiency and W Content in the Coatings

To study the influence of the cathode current density on the Faradaic efficiency (FE) and W content in coatings, we produced a set of coatings under the conditions of constant charge passed through electrolyte.

The Faradaic efficiency was estimated in accordance with

$$\eta = \eta_W + \eta_{Ni} = \frac{w_W \Delta m / E_W}{q} + \frac{w_{Ni} \Delta m / E_{Ni}}{q} \quad (3)$$

where  $\eta_W$  is the component of the FE for W,  $\eta_{Ni}$  is the component of the FE for Ni,  $E_W$  is the electrochemical equivalent for the six-valent W equal  $0.318 \times 10^{-3}$  g/C,  $E_{Ni}$  is the electrochemical equivalent for the bivalent Ni equal  $0.304 \times 10^{-3}$  g/C,  $\Delta m$  is the mass of coating (in g),  $w_W$  is the relative mass content of W in alloy,  $w_{Ni}$  is the relative mass content of Ni in alloy,  $q$  is the charge passed through electrolytes, calculated as

$$q = \int I(t)dt \quad (4)$$

where  $I$  is the working current and  $t$  is the time of deposition.

Figures 2 and 3 exhibit the dependencies of the Faradaic efficiency and W content measured in the different current modes for electrolytes with pH of 8.7 and 9.5, respectively. The relative accuracies of the FE and W content measurements were  $\pm 2.5\%$  and  $\pm 1.5\%$ , respectively.

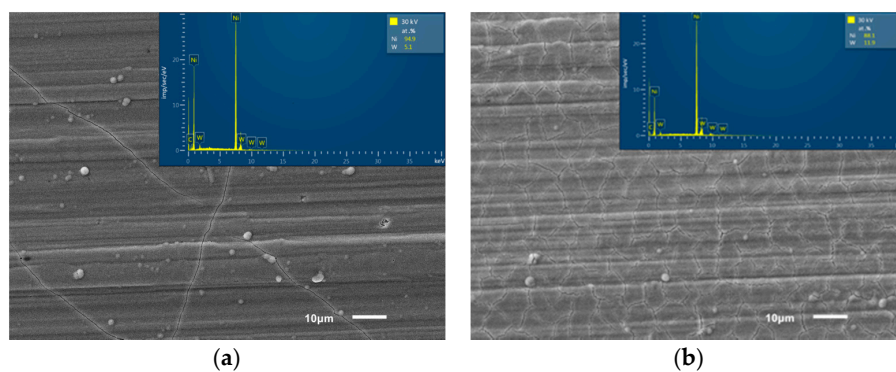


**Figure 1.** SEM images of Ni–W coatings produced in the DC mode with different current densities,  $A \cdot cm^{-2}$ : (a)  $10^{-2}$ , (b)  $5 \times 10^{-2}$ . The inset box in the upper right corner in both panels shows the EDS spectra.

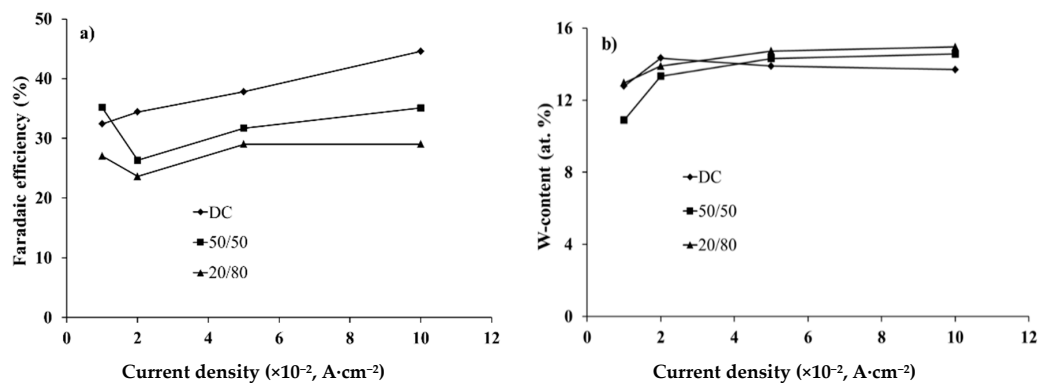


**Figure 2.** Faradaic efficiency (a), and W content (b) in Ni–W alloys versus the cathode current density in the DC and the pulse current modes with the different duty cycles (50% and 80%). The pH of the electrolyte is 8.7.

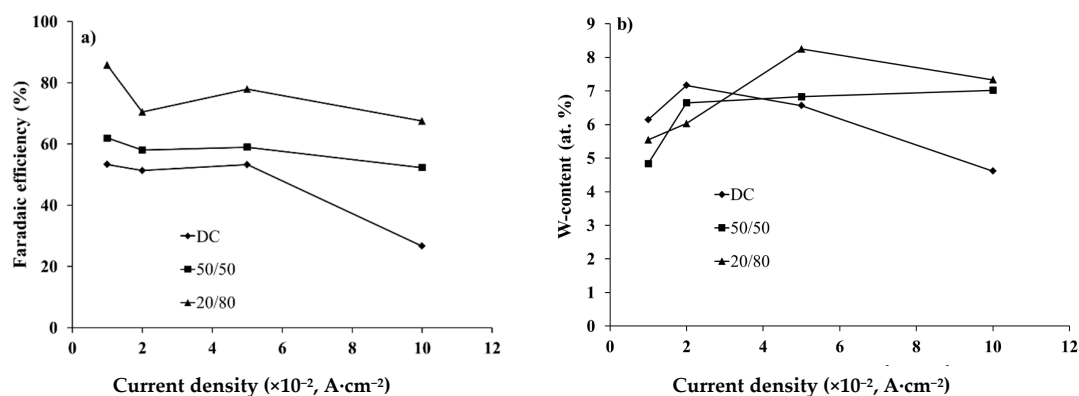


**Figure 3.** Faradaic efficiency (a), and W content (b) in Ni-W alloys versus the cathode current density in the DC and the pulse current modes with the different duty cycles (50% and 80%). The pH of the electrolytes is 9.5. For both modes a weak dependence of W content on the cathode current density was observed (Figure 2b). In comparison with the DC mode, in the pulse current mode a certain increase in W content occurs in alloy. At the same time, a decrease in the duty cycle leads to an increase in W content, which can be explained by the restoration of the concentration of W-containing ligand ions in the near-cathode layer due to their diffusion during the pauses between pulses.

For electrolytes with pH 8.7 in the PC mode, a decrease in the Faradic efficiency of 20%–30% was observed in comparison with the DC mode (Figure 2a). Within the current density of 0.02–0.1 A·cm<sup>-2</sup> for both modes, the monotonic rise of the FE values was revealed, but a decrease of the duty cycle (the relative pulse duration) results in the decreasing of FE. Such dependencies can be explained by the fact that for a pH range from 8.5 to 9.5 the Faradaic efficiency exhibits an increase, and the current density rise provokes the rise of pH in the near-cathode area. Contrariwise, a decrease of the duty cycle reduces the pH value of the electrolytes in this area.

An evident difference of the dependencies presented in Figure 2 in the range of small densities of the cathode current (0.01–0.02 A·cm<sup>-2</sup>) as against the current range discussed above indicates the transition to the other kinetics of electrochemical reactions that occurred in that range.

For an electrolyte with pH of 9.5 the FE dependencies showed a more complex character (Figure 3a). However, for both current modes they look similar: a decrease in the range of 0.01–0.02 A·cm<sup>-2</sup>, then a rise in the range of 0.02–0.05 A·cm<sup>-2</sup>, and, finally a decrease in the range of 0.05–0.1 A·cm<sup>-2</sup>. Two contrary reasons can be responsible for the maximum in the intermediate current range: on the one hand, an increase in the current density results in a rise in the pH value in the near-cathode layer, which increased the FE; on the other hand, an increase in the current density leads to the depletion of the near-cathode layer a to decrease in the concentration of ligand metal ions in it, which in turn decreases the FE. The use of the PC mode for a given electrolyte leads to an increase in the Faradaic efficiency, and its value also increases with the decreasing of the duty cycle. This can be explained by more effective restoration of the concentration of ligand metal ions in the near-cathode area due to diffusion occurring during the pauses between pulses.

For the PC mode in the current density ranging within 0.03–0.1 A·cm<sup>-2</sup>, a higher W content in the coating is achieved as compared to the DC mode (Figure 3b). A decrease in the duty cycle results in an increase of this content, and for the given experimental conditions a maximum W content of 8.2 at.% is provided at the duty cycle of 20% and the cathode current density of 0.05 A·cm<sup>-2</sup>.

When comparing the results obtained for electrolytes with pH 8.7 and 9.5, one can see that the lower pH value enables higher W content in the alloy, namely, 12–14.5 at.% as against 4.5–8.5 at.%. However, the FE of electrolytes with pH 9.5 is higher than for pH 8.7, by 2–3 times in the pulse current mode. For the DC mode the more complex character of the FE dependencies is revealed: in the range of 0.01–0.05 A·cm<sup>-2</sup> the FE for pH 9.5 increases 1.2–1.6-fold; in the range of 0.08–0.1 A·cm<sup>-2</sup> it decreases 1.4–1.8-fold.

### 3.2. Influence of the Conditions of Electrochemical Deposition on the Morphology and Microstructure of the Coatings

Figure 4 shows representative SEM images of Ni–W coatings made using electrolytes with pH 8.7 (Figure 4a) and pH 9.5 (Figure 4b). In both cases the duty cycle was chosen to be 20%, and the current density was  $0.05 \text{ A}\cdot\text{cm}^{-2}$ . The coatings possessed a characteristic metallic lustre and good adhesion to the substrate. The surface microstructure of the coatings differs. A coating produced in electrolytes with pH 8.7 (Figure 4a) exhibits microcracks and smaller numbers of separately located globules, the dimension of which ranged from  $0.5$  to  $3 \mu\text{m}$ ; in the case of electrolytes at pH 9.5 (Figure 4b) microcracks are not observed but the globular structure is more pronounced.

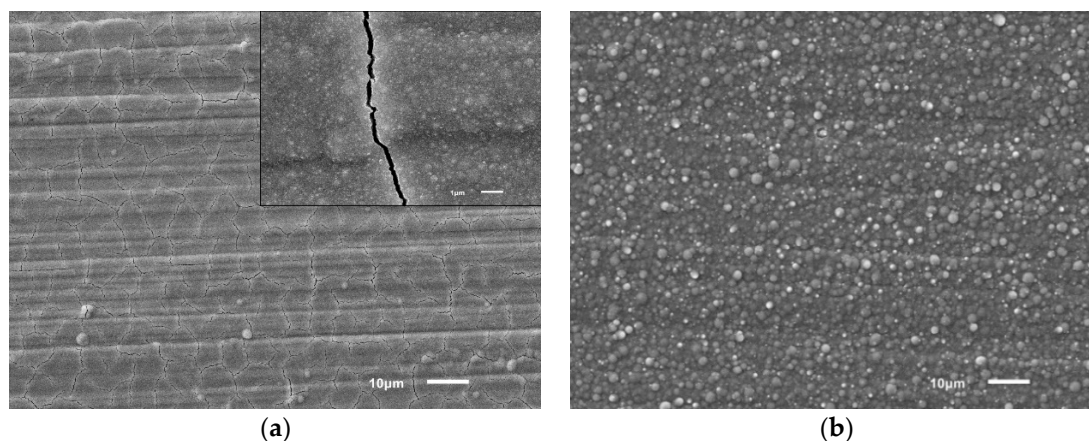


**Figure 4.** SEM images of Ni–W coatings of  $5 \mu\text{m}$  in thickness made using the PC mode in electrolytes with different pH: (a) 8.7, (b) 9.5. The inset box in the upper right corner of panel (a) shows an enlarged microcrack.

The influence of the cathode current density on coating microstructure was studied for a coating produced in electrolytes with pH 9.5 (Figure 5). An increase in the current density leads to an enlargement of the lateral dimensions of globules, from values of  $0.3$ – $1.5 \mu\text{m}$  at  $0.01 \text{ A}\cdot\text{cm}^{-2}$  to  $1$ – $3 \mu\text{m}$  at  $0.05 \text{ A}\cdot\text{cm}^{-2}$ . At that point, the number of globules slightly decreases. With a high degree of probability, this is due to the local amplification of the electric field and, correspondingly, the current density on the surface of globules, which ensures the rapid growth of their dimensions [27]. It can be mentioned that the noticeable growth of globule dimensions ceases after reaching a current density of  $0.05 \text{ A}\cdot\text{cm}^{-2}$  (Figure 5c,d). For coatings produced in electrolytes with pH 8.7, such regularity was not found. Also, the duty cycle does not contribute to a great extent to the development of surface microstructures.

At present, the mechanism of the processes responsible for the development of globular structure and the increase in the total number of globules in the course of pH changing from 8.7 to 9.5 is not clear. A rise in the rate of Ni ions' reduction in pyrophosphate electrolytes in the process of pH increasing (alkalization of electrolyte) can be considered one of the probable reasons. Also, it should be mentioned that globular structures arose as a result of the complex electrolyte ions reduction occurring on the surface of the electrode. A detailed study of the globules' formation and their further development depending on the experimental conditions will be an object of our further research.

To study phase composition and the revealing of oxides and intermetallic inclusions in Ni–W coatings, X-ray diffraction (XRD) analysis was carried out. The samples were prepared in the PC mode with different current densities using electrolytes of pH 8.7 and 9.5. The lines of Cu originating from the substrate and of the solid solution of W in Ni with f.c.c. lattice were observed, which is in agreement with the data published in [28,32]. The lines of the solid solution were significantly broadened due

to the small dimensions of the crystalline grains. Using these data, the average size of the regions of coherent scattering of Ni–W phase was estimated to be 8–10 nm for all the samples studied.

The X-ray diffraction patterns shown in Figure 6 were obtained for the Ni–W coatings produced in the PC mode using electrolytes with pH 8.7 (sample #94) and pH 9.5 (sample #96). The current density was  $0.05 \text{ A}\cdot\text{cm}^{-2}$  for both samples. One can see that the lines related to the Ni–W phase are different for these samples, and the shift of the lines is greater for those measured at bigger diffraction angles. In our opinion, this fact indicates a difference in the lattice spacing and in  $\text{Ni}_{1-x}\text{W}_x$  composition too, both of which, as found above, depend on the pH of the electrolyte. Also, no lines indicating the presence of other crystalline phases (oxides, nitrides, intermetals) were observed.

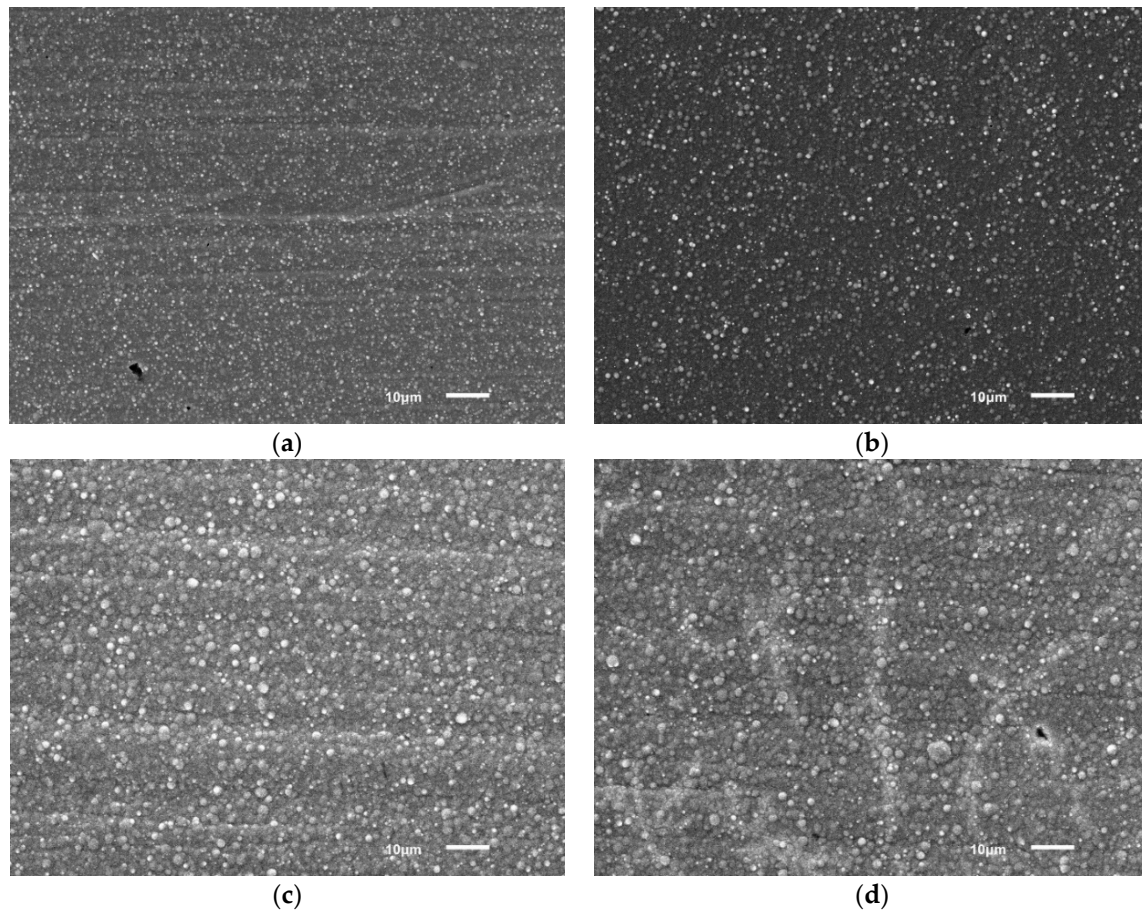


**Figure 5.** SEM images of Ni–W coatings of a 5  $\mu\text{m}$  in thickness made in electrolytes with pH 9.5 in the PC mode with different current densities,  $\text{A}\cdot\text{cm}^{-2}$ : (a) 0.01, (b) 0.02, (c) 0.05, (d) 0.1.

Post-heat treatment of the deposited coatings was not conducted in this work. In our opinion, any thermal treatment of the electrodeposited alloys of refractory metals, whether they are saturated or unsaturated solutions, can improve their mechanical properties, first of all by increasing the microhardness. In our case, the treatment of (super)saturated solid solutions causes their decomposition and the formation of a  $\text{Ni}_4\text{W}$  intermetallic phase. In turn, an increase in the microhardness of unsaturated solid solutions of tungsten occurs due to the presence of a small amount of impurities in their composition dissolved in Ni along with W. Solid solution based on f.c.c. Ni, in addition to atomic W, comprises oxygen- and hydrogen-containing impurities and represents a supersaturated solid solution. In the process of thermal treatment of such solid solution, these impurities tend to concentrate on the grain boundaries, which inhibit the movement of dislocations and result in the dispersion hardening of the coatings.

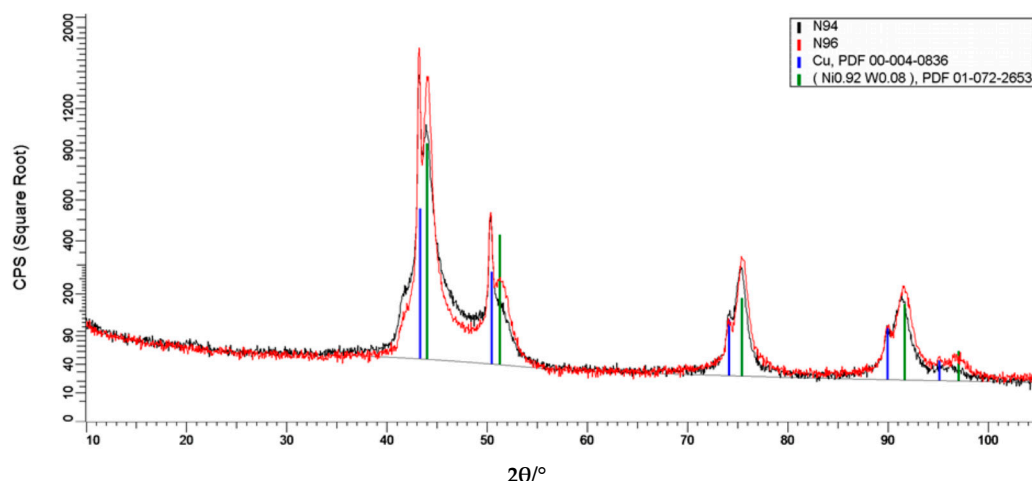


**Figure 6.** X-ray diffraction patterns obtained for Ni–W coatings produced in the pulse current mode using electrolytes with pH 8.7 (the sample #94) and pH 9.5 (the sample #96). The thickness of the coatings in both cases was 5  $\mu\text{m}$ .

### 3.3. Preparation of Crack-Free Coatings with Maximal Thickness

To study the preparation of crack-free coatings with maximum thickness, a set of samples in identical experimental conditions with a stepwise increasing deposition time for each subsequent sample was fabricated. The beginning of crack formation was determined from SEM images.

It was found that in the pulse current mode the thickness of crack-free coatings is significantly (several-fold) bigger than in the DC mode. Figure 7 shows the maximum coating thickness versus the duty cycle (the duty cycle of 100% corresponds to the DC mode). The experiments were conducted with a constant current density of  $0.05 \text{ A}\cdot\text{cm}^{-2}$  for electrolytes with pH 8.7 and 9.5, and the thickest crack-free coating was obtained for electrolytes with pH 9.5 at the duty cycle of 20%. This result can be explained by the lower hydrogen content in the coating due to its effective removal from the coating surface during the pauses between pulses.

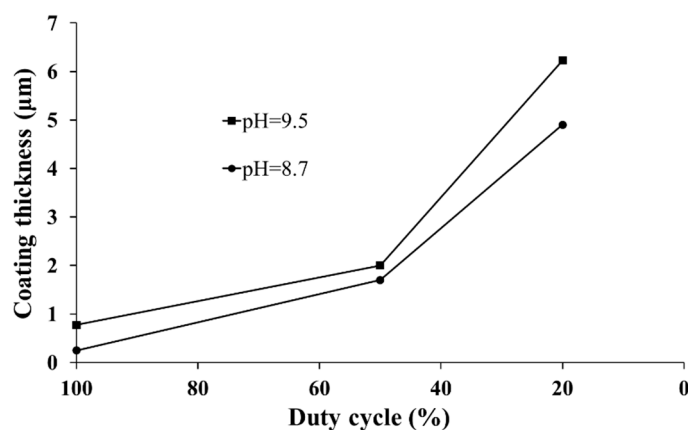


**Figure 7.** The maximum thickness of crack-free coatings versus the duty cycle (the duty cycle of 100% corresponds to the DC mode). The current density was  $0.05 \text{ A}\cdot\text{cm}^{-2}$ .

## 4. Conclusions

The conducted studies have shown that the crack-free coatings of binary Ni–W alloy with a thickness more than  $6.2 \mu\text{m}$  can be deposited using pyrophosphate electrolytes in the pulse current mode with duty cycle of up to 20%. It was found that under the experimental conditions determined in

this work, it is possible to fabricate high-quality coatings with a rather homogenous and fine-crystalline structure (crystallite dimensions of 8–10 nm) without oxides, nitrides and intermetallic inclusions.

The following conclusions and recommendations on electrochemical deposition of binary Ni–W alloy using pyrophosphate electrolytes are formulated.

- The greatest Faradaic efficiency is reached for electrolytes with a maximum stable pH value of 9.5. In that case, the optimal duty cycle is 20%.
- The greatest W content is reached for electrolytes with a lower pH value of 8.7. In that situation, the dependence of W content on the current density and duty cycle is rather weak.
- The surface morphology of coatings fabricated in electrolytes with pH 9.5 exhibits a globular structure. An increase in the current density from 0.01 to 0.05 A·cm<sup>-2</sup> leads to an increase in the dimensions of individual globules in the range from 0.3–1.5 μm to 1–3 μm, which is accompanied by a decrease in their number.

**Author Contributions:** Conceptualization and Methodology: D.V.S. and G.P.G.; Investigation: D.Y.T. and E.V.S.; Supervision: S.M.K.; Writing—Original Draft Preparation: G.P.G.; Writing—Review & Editing: A.T.

**Funding:** This research was funded by the Ministry of Education and Science of the Russian Federation in the framework of the state assignment (Project No. 11.9686.2017/8.9).

**Acknowledgments:** XRD equipment of the Centre of Physics and Technology of Micro-and Nanostructures at IPM RAS was used in this research. We thank Yurii N. Drozdov and Pavel A. Yunin for XRD data.

**Conflicts of Interest:** The authors declare no conflict of interest.

## References

1. Yamasaki, T. High-strength nanocrystalline Ni–W alloys produced by electrodeposition. *Mater. Phys. Mesh.* **2000**, *1*, 127–132.
2. Eliaz, N.; Sridhar, T.M.; Gileadi, E. Synthesis and characterization of nickel tungsten alloys by electrodeposition. *Electrochim. Acta* **2005**, *50*, 2893–2904. [[CrossRef](#)]
3. Sriraman, K.R.; Ganesh Sundara Raman, S.; Seshadri, S.K. Corrosion behavior of electrodeposited nanocrystalline Ni–W and Ni–Fe–W alloys. *Mater. Sci. Eng. A* **2007**, *460*, 39–45. [[CrossRef](#)]
4. Jones, A.; Hamann, J.; Lund, A.; Schuh, C. Nanocrystalline Ni–W alloy coating for engineering applications. *Plat. Surf. Finish.* **2010**, *97*, 52–60.
5. Wasekar, N.P.; Sundararajan, G. Sliding wear behavior of electrodeposited Ni–W alloy and hard chrome coatings. *Wear* **2015**, *342–343*, 340–348. [[CrossRef](#)]
6. Brooman, E. Corrosion performance of environmentally acceptable alternatives to cadmium and chromium coatings: Chromium-Part II. *Met. Finish.* **2000**, *98*, 39–45. [[CrossRef](#)]
7. Kirihara, S.; Umeda, Y.; Tashiro, K.; Honma, H.; Takai, O. Development of Ni–W alloy plating as a substitution of hard chromium plating. *Trans. Mater. Res. Soc. Jpn.* **2016**, *41*, 35–39. [[CrossRef](#)]
8. He, F.-J.; Wang, M.; Lu, X. Properties of electrodeposited amorphous Fe–Ni–W alloy deposits. *Trans. Nonferrous Met. Soc. China* **2006**, *16*, 1289–1294. [[CrossRef](#)]
9. Allahyarzadeh, M.H.; Aliofkhaezaei, M.; Rezvanian, A.R.; Torabinejad, V.; Sabour Rouhaghdam, A.R. Ni–W electrodeposited coatings: Characterization, properties and applications. *Surf. Coat. Technol.* **2016**, *307*, 978–1010. [[CrossRef](#)]
10. Lee, H.B. Synergy between corrosion and wear of electrodeposited Ni–W coating. *Tribol. Lett.* **2013**, *50*, 407–419. [[CrossRef](#)]
11. Udompanit, N.; Wangyao, P.; Henpraserttae, S.; Boonyongmaneerat, Y. Wear response of composition-modulated multilayer Ni–W coatings. *Adv. Mater. Res.* **2014**, *1025–1026*, 302–309. [[CrossRef](#)]
12. Amadeh, A.; Harsij Sani, M.; Moradi, H. Wear behavior of carbon steel electrodeposited by nanocrystalline Ni–W coatings. *Int. J. ISSI* **2009**, *6*, 14–19.
13. Hosseini, M.; Abdolmaleki, M.; Ebrahimzadesh, H.; Seyed Sadjadi, S. Effect of 2-butyne-1, 4-diol on the nanostructure and corrosion resistance properties of electrodeposited Ni–W–B coatings. *Int. J. Electrochem. Sci.* **2011**, *6*, 1189–1205.

14. Obradovic, M.; Stevanovic, J.; Despic, A.; Stevanovic, R.; Stoch, J. Characterization and corrosion properties of electrodeposited Ni–W alloys. *J. Serb. Chem. Soc.* **2001**, *66*, 899–912. [[CrossRef](#)]
15. Chianpairot, A.; Lothongkum, G.; Schuh, C.A.; Boonyongmaneerat, Y. Corrosion of nanocrystalline Ni–W alloys in alkaline and acidic 3.5 wt.% NaCl solutions. *Cor. Sci.* **2011**, *53*, 1066–1071. [[CrossRef](#)]
16. Alimadadi, H.; Ahmadi, M.; Aliofkhaezai, M.; Younesi, S.R. Corrosion properties of electrodeposited nanocrystalline and amorphous patterned Ni–W alloy. *Mater. Des.* **2009**, *30*, 1356–1361. [[CrossRef](#)]
17. Yang, Y.; Zhang, Y.; Zhang, Y.; Yan, B.; Mo, F. Corrosion properties of ultrasonic electrodeposited nanocrystalline and amorphous patterned Ni–W alloy coatings. *Mod. Phys. Lett. B* **2013**, *27*, 1341007. [[CrossRef](#)]
18. Sassi, W.; Dhoubi, L.; Berçot, P.; Rezrazi, M.; Triki, E. Effect of pyridine on the electro-crystallization and corrosion behavior of Ni–W alloy coated from citrate-ammonia media. *Appl. Surf. Sci.* **2012**, *263*, 373–381. [[CrossRef](#)]
19. Yang, F.Z.; Guo, Y.F.; Huang, L.; Xu, S.K.; Zhou, S.M. Electrodeposition, structure and corrosion resistance of nanocrystalline Ni–W alloy. *Chin. J. Chem.* **2004**, *22*, 228–231. [[CrossRef](#)]
20. Metikoš-Huković, M.; Grubač, Z.; Radić, N.; Tonejc, A. Sputter deposited nanocrystalline Ni and Ni–W films as catalysts for hydrogen evolution. *J. Mol. Catal. A Chem.* **2006**, *249*, 172–180. [[CrossRef](#)]
21. Hristova, E.; Mitov, M.; Rashkov, R.; Arnaudova, M.; Popov, A. Sulphide oxidation on electrodeposited Ni–Mo–W catalysts. *Bulg. Chem. Commun.* **2008**, *40*, 291–294.
22. Kawashima, A.; Akiyama, E.; Habazaki, H.; Hashimoto, K. Characterization of sputter deposited Ni–Mo and Ni–W alloy electrocatalysts for hydrogen evolution in alkaline solution. *Mater. Sci. Eng. A* **1997**, *226*, 905–909. [[CrossRef](#)]
23. Do, T.K.; Lund, A. A reliability study of a new nanocrystalline nickel alloy barrier layer for electrical contacts. In Proceedings of the 56th IEEE Holm Conference on Electric Contacts, Charleston, SC, USA, 4–7 October 2010; pp. 73–81.
24. Mizushima, I.; Tang, P.T.; Hansen, H.N.; Somers, M.A. Residual stress in Ni–W electrodeposits. *Electrochim. Acta* **2006**, *51*, 6128–6134. [[CrossRef](#)]
25. Wang, M.; Wang, Z.; Guo, Z. The structure evolution and stability of Ni–W films electrodeposited under super gravity field. *Mater. Lett.* **2010**, *64*, 1166–1168. [[CrossRef](#)]
26. Zemanova, M.; Krivosudska, M.; Chovancova, M.; Jorik, V. Pulse current electrodeposition and corrosion properties of Ni–W alloy coatings. *J. Appl. Electrochem.* **2011**, *41*, 1077–1085. [[CrossRef](#)]
27. Vasko, A.T. *Electrochemistry of Molybdenum and Tungsten*; Naukova Dumka: Kiev, Ukraine, 1977; p. 172. (In Russian)
28. Krasikov, A.V.; Krasikov, V.L. Mechanism of nickel-tungsten alloy electrodeposition from pyrophosphate electrolyte. *Bull. SPbSTI* **2016**, *36*, 12–23. (In Russian) [[CrossRef](#)]
29. Nirmal Peiris, T.A.; Senthilarasu, S.; Upul Wijayantha, K.G. Enhanced performance of flexible dye-sensitized solar cells: Electrodeposition of Mg(OH)<sub>2</sub> on nanocrystalline TiO<sub>2</sub> electrode. *J. Phys. Chem. C* **2012**, *116*, 1211–1218. [[CrossRef](#)]
30. Suvorov, D.V.; Gololobov, G.P.; Tolstoguzov, A.B.; Karabanov, S.M.; Tarabrin, D.Y.; Rybin, N.B.; Stryuchkova, Y.M.; Serpova, M.A.; Korotchenko, V.A. Electrodeposition of Ni–W gradient coatings. *J. Phys. Conf. Ser.* **2017**, *857*, 012047. [[CrossRef](#)]
31. Zhu, L.; Younes, O.; Ashkenasy, N.; Shacham-Diamand, Y.; Gileadi, E. STM/AFM studies of the evolution of morphology of electroplated Ni/W alloys. *Appl. Surf. Sci.* **2002**, *200*, 1–14. [[CrossRef](#)]
32. Lyakishev, N.P. *Diagrams of the State of Double Metal Systems*; Mashinostroenie: Moscow, Russia, 2001; p. 872. (In Russian)

